Excessive tau accumulation in the parieto-occipital cortex characterizes early-onset Alzheimer's disease

Hanna Cho

Department of Medicine

The Graduate School, Yonsei University

Excessive tau accumulation in the parieto-occipital cortex characterizes early-onset Alzheimer's disease

Directed by Professor Young-Chul Choi

The Doctoral Dissertation
submitted to the Department of Medicine,
the Graduate School of Yonsei University
in partial fulfillment of the requirements
for the degree of Doctor of Philosophy

Hanna Cho

June 2017

연세대학교
YONSEI UNIVERSITY

This certifies that the Doctoral Dissertation
of Hanna Cho is approved.

Thesis Supervisor : Young-Chul Choi

Thesis Committee Member#1 : Chul Hyoung Lyoo

Thesis Committee Member#2 : Kook In Park

Thesis Committee Member#3 : Yun Joong Kim

Thesis Committee Member#4 : Chul Hoon Kim

The Graduate School
Yonsei University

June 2017

ACKNOWLEDGEMENTS

I would like to offer my deepest thanks to Prof. Young-Chul Choi for his constant concern and worthy guidance in helping me complete this thesis. I really appreciate Prof. Chul Hyoung Lyoo for teaching me the pleasure of research in this study. I also thank Prof. Kook In Park, Yun Joong Kim, and Chul Hoon Kim for their valuable advice and critical comments on this study. I would like to dedicate this thesis to my beloved family (parents, husband, Beom Jun, and Beom Seo) who fully supported and trusted me. Lastly, I thank God for the meaning of my existence.

<TABLE OF CONTENTS>

ABSTRACT 1
I. INTRODUCTION 2
II. MATERIALS AND METHODS 3
1. Participants 3
2. Neuropsychological tests 4
3. Image acquisition and processing 4
A. Acquisition of PET and MR images 4
B. Image processing steps 4
4. Statistical analysis 6
III. RESULTS 7
1. Demographic characteristics 7
2. Comparison of cortical ^{18}F-AV-1451 binding 8
3. Surface-based comparison of cortical ^{18}F-AV-1451 binding 11
4. Association between cognitive function and cortical ^{18}F-AV-1451 binding 13
5. Comparison of cortical ^{18}F-florbetaben binding and correlation with cognitive function 17
IV. DISCUSSION 19
V. CONCLUSION 20

REFERENCES 21
ABSTRACT (IN KOREAN) 25
PUBLICATION LIST 27

LIST OF FIGURES

Figure 1. Surface-based comparisons of ^{18}F-AV-1451 binding ……..……..12
Figure 2. Surface-based correlation analysis between ^{18}F-AV-1451 binding and cognition in early- and late-onset patients with Alzheimer's disease spectrum...15
Figure 3. Correlation between ^{18}F-AV-1451 binding values and cognition in early- and late-onset patients with Alzheimer's disease spectrum……..16

LIST OF TABLES

Table 1. Demographic characteristics of each group.....7
Table 2. Comparison of ^{18}F-AV-1451 binding values between the diagnostic groups……..…….……9
Table 3. An interaction analysis between the onset age (young and old) and the diagnostic groups (controls, MCI, and AD) in ^{18}F-AV-1451 binding values.....10
Table 4. Correlation between the ^{18}F-AV-1451 binding values and cognition in early- and late-onset patients with Alzheimer's disease spectrum…….....14
Table 5. Comparison of ^{18}F-florbetaben binding values between the diagnostic groups…….…….…18

ABSTRACT

Excessive tau accumulation in the parieto-occipital cortex characterizes early-onset Alzheimer's disease

Hanna Cho

Department of Medicine
The Graduate School, Yonsei University

(Directed by Professor Young-Chul Choi)

Background: Early-onset Alzheimer's disease (EOAD) is associated with a greater impairment of various non-memory functions, more rapid progression, and greater cortical hypometabolism and atrophy when compared to late-onset AD (LOAD) even when similar amyloid-β burden was present in positron emission tomography (PET) studies. We sought to investigate the differences in topographical patterns of tau accumulation between the early- and late-onset patients with AD and mild cognitive impairment (MCI). **Methods:** In 90 amnestic MCI and mild to moderate AD patients who completed ^{18}F-AV-1451 and ^{18}F-florbetaben positron emission tomography scans, 59 amyloid-positive patients were included (11 EOAD, 10 EOMCI, 21 LOAD, and 17 LOMCI). We compared cortical ^{18}F-AV-1451 and ^{18}F-florbetaben binding between each patient group and corresponding amyloid-negative age-matched controls. **Results:** Compared to each control group, both EOAD and LOAD groups showed markedly increased ^{18}F-AV-1451 binding across the entire neocortex, while only the LOMCI group showed increased binding in the medial temporal cortex. In contrast to no difference in cortical ^{18}F-AV-1451 binding between the EOMCI and LOMCI, the EOAD showed greater ^{18}F-AV-1451 binding in the parieto-occipital cortex than LOAD. The parieto-occipital ^{18}F-AV-1451 binding correlated with the visuospatial dysfunction in EOAD spectrum, while the binding in the temporal cortex correlated with verbal memory dysfunction in LOAD spectrum. Cortical ^{18}F-florbetaben binding did not differ between the EOAD and LOAD groups. **Conclusion:** EOAD patients have a greater tau burden, particularly in the parieto-occipital cortex than LOAD patients. Distinct topographic distribution of tau may influence the nature of cognitive impairment in EOAD patients.

Key words: Alzheimer's disease; mild cognitive impairment; early onset; tau; positron emission tomography

Excessive tau accumulation in the parieto-occipital cortex characterizes early-onset Alzheimer's disease

Hanna Cho

Department of Medicine
The Graduate School, Yonsei University

(Directed by Professor Young-Chul Choi)

Ⅰ. INTRODUCTION

Early-onset Alzheimer's disease (EOAD) has a greater impact on occupational and socio-economic status [1], undergoes more rapid progression, and is associated with a shorter survival period than late-onset AD (LOAD) [2,3]. EOAD is also characterized by greater impairment of various non-memory functions including attention, visuospatial, language, praxis, and executive functions than LOAD, which is predominantly associated with memory impairment [3-6]. Accompanying these distinct patterns of neuropsychological dysfunction, EOAD patients show more severe hypometabolism and cortical atrophy, particularly in the parietal, posterior cingulate and precuneus cortices [5,7-9].

Postmortem pathological studies have reported greater burden of amyloid-β plaques and neurofibrillary tangles (NFT) in the parieto-frontal association cortices of EOAD patients than in LOAD patients [10,11]. In a study using a cut-off of 62 years, EOAD patients showed greater ^{11}C-Pittsburgh Compound B (PIB) binding in the parietal cortex than LOAD patients [12]. However, unlike these postmortem and in vivo imaging studies, no difference in cortical ^{11}C-PIB binding has been shown between EOAD and LOAD patients dichotomized by the age cut-off of 65 years at onset [7,13].

^{18}F-AV-1451 is a recently developed radiotracer specific for paired helical filaments (PHF) of hyperphosphorylated tau protein [14], and enables the in vivo visualization of tau pathology [15]. Cortical ^{18}F-AV-1451 binding patterns clearly mirror the known topographic distribution of neurofibrillary tangle (NFT) pathology in AD [16,17].

In the present study, we sought to investigate differences in ^{18}F-AV-1451 binding patterns between early- and late-onset patients with AD and mild cognitive impairment (MCI). We also investigated the cortical regions in which ^{18}F-AV-1451 binding correlates with specific neuropsychological function in each age-related group.

Ⅱ. MATERIALS AND METHODS

1. Participants

This study was approved by the Institutional Review Board of Gangnam Severance Hospital, and written informed consent was obtained from all participants.

Between January 2015 to Feb 2016, 90 MCI and mild to moderate AD dementia patients who had been clinically diagnosed at the Memory Disorder Clinic of Gangnam Severance Hospital were recruited. Clinical interviews, neurological examination, laboratory blood tests, apolipoprotein E (APOE) genotyping, neuropsychological tests, conventional brain magnetic resonance (MR) imaging, and ^{18}F-florbetaben (for amyloid-β) and ^{18}F-AV-1451 (for tau) PET scans were conducted for all patients.

AD patients were required to meet the criteria for probable AD as proposed by the National Institute of Neurological and Communicative Disorders and Stroke and the Alzheimer's Disease and Related Disorders Association (NINCDS-ADRDA) [18]. Amnestic MCI was diagnosed based on Petersen's criteria [19]; performance of verbal or visual memory function tests below -1.5 SD of age- and education-adjusted norm. Patients were excluded if they exhibited other structural lesions identified by brain MRI, including territorial infarction, intracranial hemorrhage, brain tumor, hydrocephalus, or severe white matter hyperintensities (Fazekas scale 3) [20]. Potential secondary causes of cognitive deficits were excluded by additional laboratory tests including complete blood count, blood chemistry, vitamin B12, folate, syphilis serology, and thyroid function tests. We also excluded patients who met the diagnostic criteria for psychotic or mood disorders such as schizophrenia or major depressive disorder. There were no patients presenting with atypical features suggesting AD variants (posterior cortical atrophy, logopenic aphasia, or frontal-variant AD). Although we could not perform any genetic tests other than apolipoprotein E genotyping, none of the patients had a family history suspicious for autosomal dominant AD; ≥ 2 first degree relatives with a history of dementia or ≥ 1 family member presenting dementia in extremely young age.

The controls were healthy volunteers with no history of neurological or psychiatric illness and no abnormalities detected by neurological examination. All control subjects underwent the same neuropsychological tests and neuroimaging studies as the patients. All showed normal cognition (above -1.5 SD of age- and education-adjusted norm) on detailed neuropsychological tests.

Using the visual assessment method validated with postmortem tissue [21,22], amyloid-positivity was determined by two nuclear medicine specialists (Y.H.R. and J.H.L.) who were blinded to the clinical diagnosis. Onset ages were determined by an interview conducted with family members or caregivers. The patients were divided into subgroups according to the age cut-off of 65 years at onset, with 30 patients in the early-onset AD spectrum (EOAD/MCI: onset age < 65 years; 12 EOAD and 18 EOMCI) and 60 patients in the late-onset AD spectrum (LOAD/MCI: onset age ≥ 65 years; 31 LOAD and 29

LOMCI). For this study, we finally included amyloid-positive patients: 11/12 (91.7%) EOAD, 10/18 (55.6%) EOMCI, 21/31 (67.7%) LOAD, and 17/29 (58.7%) LOMCI.

For comparison of the AD/MCI groups, two age-matched control groups comprising 15 young controls (YC) and 15 old controls (OC) negative for amyloid were included.

2. Neuropsychological tests

All subjects underwent neuropsychological tests using a standardized battery called the Seoul Neuropsychological Screening Battery [23,24]. We assessed attention (Digit Span Backward: DS-BW), language (Boston Naming Test: BNT), visuospatial/constructive (Rey-Osterrieth Complex Figure Test: RCFT), verbal memory (Seoul Verbal Learning Test-Delayed Recall: SVLT-DR), visual memory (Rey-Osterrieth Complex Figure Test-Delayed Recall: RCFT-DR), frontal/executive functions (Controlled Oral Word Association Test-Semantics: COWAT), and Clinical Dementia Rating sum-of-boxes (CDR-SB), and also conducted the Mini-Mental State Examination (MMSE).

3. Image acquisition and processing

A. Acquisition of PET and MR images

All PET images were acquired using a Biograph mCT PET/CT scanner (Siemens Medical Solutions; Malvern, PA, USA). We intravenously injected 281.2 ± 35.2 MBq of ^{18}F-AV-1451 for tau PET and 297.9 ± 34.5 MBq of ^{18}F-florbetaben for amyloid PET. Prior to the PET scans, a head holder was applied to minimize head motion and brain CT images were acquired for attenuation correction. At 80 mins after the injection of ^{18}F-AV-1451 and at 90 mins after the injection of ^{18}F-florbetaben, PET images were acquired for 20 mins. After correcting for attenuation, scatter and decay, 3D PET images were finally reconstructed with the ordered-subsets expectation maximization (OSEM) algorithm in a 256×256×223 matrix with 1.591×1.591×1 mm voxel size.

Axial T1-weighted brain MR images were obtained with 3D-spoiled gradient-recalled sequences (3D-SPGR sequences; repetition time = 8.28 ms, echo time = 1.6 to 11.0 ms, flip angle = 20°, 512×512 matrix, voxel size 0.43×0.43×1 mm) in a 3.0 Tesla MR scanner (Discovery MR750, GE Medical Systems, Milwaukee, WI).

B. Image processing steps

We used FreeSurfer 5.3 (Massachusetts General Hospital, Harvard Medical School; http://surfer.nmr.mgh.harvard.edu) and in-house software implemented in MATLAB 7.1 (MathWorks) for the processing of T1-weighted brain MR images and creating participant-specific volume-of-interest (VOI) masks. Subcortical structures were segmented after inhomogeneity correction and segmentation of MR images into gray and white matter by using

the intensity gradient across the layers and connectivity between the voxels. After tessellation with more than 100,000 vertices of trigons, 3D-surfaces for cortical gray matter and white matter were obtained. Cortical thickness (defined as the distance between the gray matter surface and corresponding white matter surface) was measured, and the thickness values and curvature information for each vertex were overlaid onto the white matter surface.

Subcortical gray matter structures were labelled by probabilistic registration technique to create VOI masks for subcortical regions.[25] By using a surface-based probabilistic labelling algorithm based on the curvature information on white matter surface, cerebral cortical regions were parcellated, and cortical VOI masks were created.[26,27] A composite VOI mask containing 112 regions was created by merging cortical and subcortical VOI masks. We merged anatomically related regions to create a VOI mask image with 36 cortical and subcortical regions. With this final VOI mask image, we corrected for the partial volume effect (PVE) using the region-based voxel-wise (RBV) method,[28] and measured regional volumes using the voxel counts within each VOI mask. The cerebellar cortex was used as a reference region to create standardized uptake value ratio (SUVR) images. Finally, we measured PVE-uncorrected and corrected regional SUVR values for 25 cortical regions (inferior, middle and superior frontal, orbitofrontal, paracentral, precentral, inferior and superior parietal, postcentral, precuneus, supramarginal, medial and lateral occipital, lingual, insula, inferior, middle and superior temporal, fusiform, parahippocampal, anterior and posterior cingulate cortices, amygdala, and hippocampus).

For the surface-based visualization and statistical analysis of PET images, standardized uptake values (SUV) of the voxels at the mid-point between the gray and white matter surface for each vertex was assigned for each vertex. A surface-based SUVR map was created with the cerebellar cortex SUVs obtained by volume-based approach and spatially normalized to the average surface. The spatially normalized surface-based SUVR maps were then convoluted by Gaussian kernel with 8 mm full-width half maximum (FWHM) to reduce noise. Similarly, cortical thickness maps overlaid on the white matter surface were spatially normalized and smoothed for the later statistical comparison.

We primarily used VOI data uncorrected for partial volume effect, but additionally analyzed VOI data corrected for partial volume effect by using the region-based voxel-wise partial volume correction method [28].

4. Statistical analysis

Demographic data was analyzed using ANOVA and post-hoc comparison for continuous variables and chi-square test for categorical variables. For the comparison of neuropsychological tests, we first used the analysis of covariance (ANCOVA) model with years of education as covariates, and then corrected multiple comparisons of each between-group comparison with the Bonferroni method. We primarily compared between the young and corresponding old groups (e.g. EOAD *vs.* LOAD, EOMCI *vs.* LOMCI, and YC *vs.* OC).

We performed interaction analysis by using the general linear model adjusting for the year of education to observe the interaction of regional ^{18}F-AV-1451 binding values between the onset age (early- and late-onset) and diagnosis (healthy control, MCI and AD) and also between the onset age and the MMSE score. For the between-group comparison, we compared regional ^{18}F-AV-1451 SUVR values between the three diagnostic groups in EOAD/MCI and LOAD/MCI separately by using the ANCOVA model with age and years of education as covariates. For the group comparisons between the EO and LO groups (EOAD *vs.* LOAD and EOMCI *vs.* LOMCI), we used years of education and MMSE as covariates. Bonferroni's correction was used to correct for the multiple comparisons of each between-group comparison, and region-wise multiple comparisons were corrected by using Benjamini-Hochberg's false discovery rate (FDR) method [29]. With the same method, we also compared ^{18}F-florbetaben SUVR values between the groups.

For the correlation analysis between the global cognitive scale (MMSE scores) and regional ^{18}F-AV-1451 SUVR values in EOAD/MCI and LOAD/MCI separately, we first obtained standardized residuals of global cognitive scales and regional SUVR values adjusted for age and years of education by using a general linear model and then ran Pearson's correlation between the standardized residuals of global cognitive scales and regional SUVR values. Likewise, the correlation between the tests for each cognitive domain and regional SUVR values was analysed after controlling for age, years of education and MMSE score. We performed all statistical analyses using SPSS 23 (IBM Corp., Armonk, NY).

We used the FreeSurfer software for the surface-based statistical analysis. Similar to the VOI-based analysis, we compared the cortical ^{18}F-AV-1451 binding between the groups by using the general linear model with the covariates used for the corresponding VOI-based comparison. Also, by using the general linear model with the same covariates used for the VOI-based correlation analysis, we performed correlation analysis between cognitive performance and cortical binding. Vertices with FDR-corrected $P < 0.05$ were considered to be significant.

Ⅲ. RESULTS

1. Demographic characteristics

Except for younger ages and/or ages-at-onset in the younger groups (EOAD, EOMCI and YC) in comparison to the older groups (LOAD, LOMCI and OC), each younger group was not statistically different in terms of gender, education, duration of disease, frequency of ApoE ε4 genotype, MMSE, or CDR-SB from their corresponding older group. The EOAD patients performed worse on the visuospatial function test (RCFT) than the LOAD patients, while LOAD performed worse on the language function test (BNT). OC performed worse on the visual memory function than YC. Detailed demographic and clinical data of the participants are presented in Table 1.

Table 1. Demographic characteristics of each group

	EOAD/MCI		YC	LOAD/MCI		OC
	EOAD	**EOMCI**		**LOAD**	**LOMCI**	
n	11	10	15	21	17	15
Age (years)	64.8 ± 3.8*	63.2 ± 6.4*	64.3 ± 1.9*	78.6 ± 5.2	76.5 ± 5.9	76.5 ± 6.0
Onset age (years)	60.6 ± 2.9*	60.0 ± 5.4*	n.a	74.6 ± 5.3	73.9 ± 5.9	n.a
Gender (M : F)	3 : 8	5 : 5	4 : 11	2 : 19	8 : 9	6 : 9
Education (years)	13.3 ± 5.3	12.4 ± 4.7	10.3 ± 4.2	9.1 ± 5.9	10.7 ± 5.1	9.8 ± 6.2
Duration (years)	3.6 ± 1.3	3.0 ± 1.3	n.a	4.0 ± 1.8	2.6 ± 0.6	n.a
ApoE ε4 genotype (%)	7/11 (63.6)	4/10 (40.0)	2/15 (13.3)	11/20 (55.0)	9/17 (52.9)	2/15 (13.3)
Use of AchE inhibitor	11 / 11	8 / 10	n.a.	21 / 21	13 / 17	n.a.
Use of memantine	6 / 11	0 / 10	n.a.	9 / 21	2 / 17	n.a.
MMSE	18.4 ± 3.7	25.6 ± 2.5	28.1 ± 1.7	19.1 ± 4.4	24.7 ± 3.3	27.0 ± 2.1
CDR-SB	5.7 ± 2.8	1.7 ± 0.9	0	4.8 ± 1.5	2.1 ± 1.0	0
DS-BW	2.5 ± 1.5	4.1 ± 2.3	3.9 ± 1.0	2.6 ± 1.7	3.3 ± 1.0	3.2 ± 0.8
BNT	39.2 ± 10.3	46.1 ± 5.2	50.3 ± 5.8	28.0 ± 9.5*	39.2 ± 6.1	47.5 ± 8.0
RCFT	15.7 ± 12.8*	32.7 ± 3.5	33.6 ± 2.1	22.1 ± 10.1	29.1 ± 7.7	30.9 ± 5.6
SVLT-DR	0.7 ± 2.4	1.7 ± 1.8	6.7 ± 2.0	0.3 ± 0.9	0.6 ± 1.1	5.7 ± 2.0
RCFT-DR	0.5 ± 1.3	6.7 ± 6.5	18.4 ± 4.6	1.8 ± 2.6	4.7 ± 5.7	10.0 ± 4.9*
COWAT	8.0 ± 3.4	12.5 ± 3.9	17.0 ± 4.3	8.8 ± 2.9	11.5 ± 6.0	14.6 ± 4.9

*$P < 0.05$ for the comparisons between each young group and corresponding old group (e.g. EOAD *vs.* LOAD, EOMCI *vs.* LOMCI, and YC *vs.* OC)

Abbreviations: EO = early-onset; LO = late-onset; AD/MCI = Alzheimer's disease spectrum; AD = Alzheimer's disease; MCI = mild cognitive impairment; YC = young controls; OC = old controls; ApoE = apolipoprotein E; MMSE = Mini-Mental State Examination; CDR-SB = Clinical Dementia Rating sum-of-boxes; DS-BW = Digit Span Backward; BNT = Boston Naming Test; RCFT = Rey-Osterrieth Complex Figure Test; SVLT-DR = Seoul Verbal Learning Test-Delayed Recall; RCFT-DR = Rey-

Osterrieth Complex Figure Test-Delayed Recall; COWAT = Controlled Oral Word Association Test-Semantics; n.a. = not applicable

2. Comparison of cortical ^{18}F-AV-1451 binding

Regional SUVR values of ^{18}F-AV-1451 PET and the statistical results are summarized in Table 2 and Table 3. The interaction between the onset age (early- and late-onset) and diagnosis (healthy control, MCI and AD) was tested at a significance level of 0.05, and we found interactions between the onset age and diagnosis in the superior and inferior parietal, precuneus, occipital, superior and inferior temporal, and parahippocampal cortices (Table 3). Therefore, for the post-hoc analysis, we separately analyzed group-wise comparisons (Table 2). The EOMCI patients showed greater ^{18}F-AV-1451 binding than YC only in the entorhinal cortex (P = 0.030). However, this region did not survive region-wise multiple comparisons. The LOMCI patients showed greater binding than OC in the inferior parietal, middle and inferior temporal, hippocampus, entorhinal, and parahippocampal cortices. Only the entorhinal (P < 0.001) and parahippocampal (P = 0.004) cortices survived multiple comparisons. Both EOAD and LOAD patients showed greater ^{18}F-AV-1451 binding than each age-matched control group in all cortical regions (Table 2).

With the exception of the hippocampus, the EOAD patients showed greater binding than the EOMCI patients in most of the cortical regions. Compared with LOMCI, the LOAD patients showed greater global cortical binding (P = 0.029). Additionally, binding in the prefrontal (P = 0.040), precuneus (P = 0.008), and anterior (P = 0.040) and posterior (P = 0.039) cingulate cortices of LOAD patients was greater than those for LOMCI. However, none of the regions survived multiple comparisons (Table 2).

Cortical ^{18}F-AV-1451 binding did not differ between the EOMCI and LOMCI patients. In contrast, the EOAD patients showed greater binding in the superior and inferior parietal, and occipital cortices (P < 0.010), and hippocampus (P = 0.039) compared to the LOAD patients. Only the hippocampus failed to survive multiple comparisons (Table 2). Even after correcting for the partial volume effect, the statistical outcomes were not different from those of uncorrected data.

We also investigated correlation analysis between the regional ^{18}F-AV-1451 binding and ages at onset in all 59 AD/MCI patients with the years of education and MMSE scores as covariates. The ^{18}F-AV-1451 binding in the global cortex negatively correlated with the onset age (P = 0.008), and similar to the EOAD *vs.* LOAD comparison, binding in the superior and inferior parietal (P = 0.003), precuneus (P = 0.013), and occipital (P = 0.024) cortices negatively correlated with the onset age even after controlling for region-wise multiple comparisons.

When we lowered cut-off onset age to 62 years for classifying EO- and LOAD/MCI patients, LOMCI patients showed greater ^{18}F-AV-1451 binding in the widespread temporal cortex than EOMCI patients. Conversely, EOAD patients showed still greater ^{18}F-AV-1451 binding in widespread fronto-parieto-occipital cortices than LOAD patients.

Table 2. Comparison of ^{18}F-AV-1451 binding values between the diagnostic groups

	SUVR			***P*-value**			
	EOAD	**EOMCI**	**YC**	**EOAD > YC**	**EOMCI > YC**	**EOAD > EOMCI**	**EOMCI > LOMCI**
Global cortex	1.71±0.39	1.25±0.27	1.12±0.07	***< 0.001***	> 0.999	***0.001***	0.750
Prefrontal	1.63±0.41	1.26±0.28	1.16±0.09	***0.001***	> 0.999	***0.007***	0.535
Sensorimotor	1.36±0.31	1.10±0.16	1.05±0.09	***0.002***	> 0.999	***0.006***	0.430
Superior parietal	1.84±0.63	1.22±0.28	1.07±0.10	***< 0.001***	> 0.999	***0.001***	0.328
Inferior parietal	2.05±0.68	1.34±0.42	1.10±0.10	***< 0.001***	> 0.999	***0.002***	0.414
Precuneus	2.00±0.69	1.36±0.40	1.13±0.10	***< 0.001***	> 0.999	***0.004***	0.334
Occipital	1.57±0.29	1.16±0.17	1.09±0.08	***< 0.001***	> 0.999	***< 0.001***	0.972
Superior	1.61±0.41	1.17±0.22	1.06±0.08	***< 0.001***	> 0.999	***0.001***	0.877
Middle temporal	1.95±0.48	1.38±0.41	1.14±0.07	***< 0.001***	0.472	***0.003***	0.807
Inferior temporal	2.10±0.54	1.37±0.36	1.14±0.06	***< 0.001***	0.595	***< 0.001***	0.627
Hippocampus	1.64±0.20	1.40±0.29	1.24±0.13	***< 0.001***	0.079	0.084	0.660
Entorhinal	1.91±0.27	1.50±0.49	1.17±0.08	***< 0.001***	***0.030****	***0.024***	0.247
Parahippocampal	1.83±0.24	1.33±0.34	1.11±0.06	***< 0.001***	0.061	***< 0.001***	0.386
Anterior	1.43±0.22	1.21±0.17	1.18±0.10	***0.002***	> 0.999	***0.009***	0.991
Posterior	1.84±0.46	1.34±0.34	1.14±0.08	***< 0.001***	0.712	***0.002***	0.728
	SUVR			***P*-value**			
	LOAD	**LOMCI**	**OC**	**LOAD > OC**	**LOMCI > OC**	**LOAD > LOMCI**	**EOAD > LOAD**
Global cortex	1.38±0.22	1.24±0.14	1.11±0.08	***< 0.001***	0.120	***0.029***	***0.043***
Prefrontal	1.40±0.35	1.21±0.13	1.15±0.07	***0.006***	> 0.999	***0.040****	0.354
Sensorimotor	1.15±0.12	1.06±0.12	1.03±0.08	***0.009***	> 0.999	0.065	0.086
Superior parietal	1.27±0.22	1.14±0.17	1.03±0.11	***0.001***	0.238	0.163	***0.006***
Inferior parietal	1.40±0.24	1.26±0.17	1.08±0.12	***< 0.001***	***0.037****	0.096	***0.004***
Precuneus	1.48±0.33	1.25±0.19	1.14±0.09	***< 0.001***	0.617	***0.008****	0.053
Occipital	1.25±0.16	1.16±0.16	1.07±0.10	***0.005***	0.240	0.376	***0.003***
Superior	1.31±0.23	1.20±0.19	1.05±0.09	***< 0.001***	0.090	0.210	0.053
Middle temporal	1.62±0.39	1.44±0.30	1.14±0.08	***< 0.001***	***0.020****	0.200	0.192
Inferior temporal	1.66±0.37	1.44±0.25	1.16±0.08	***< 0.001***	***0.019****	0.075	0.061
Hippocampus	1.48±0.22	1.47±0.28	1.26±0.22	***0.031***	***0.043****	> 0.999	***0.039****
Entorhinal	1.78±0.31	1.72±0.36	1.22±0.18	***< 0.001***	***< 0.001***	> 0.999	0.355
Parahippocampal	1.61±0.29	1.45±0.28	1.15±0.11	***< 0.001***	***0.004***	0.200	0.060
Anterior	1.40±0.33	1.22±0.13	1.17±0.09	***0.010***	> 0.999	***0.040****	0.959
Posterior	1.52±0.37	1.30±0.24	1.16±0.09	***0.001***	0.408	***0.039****	0.152

*Regions did not survive region-wise correction for multiple comparisons.

Data are presented as mean ± SD.

Abbreviations: SUVR = standardized uptake value ratio; EO = early-onset; LO = late-onset; AD/MCI = Alzheimer's disease spectrum; AD = Alzheimer's disease; MCI = mild cognitive impairment; YC = young controls; OC = old controls

Table 3. An interaction analysis between the onset age (young and old) and the diagnostic groups (controls, MCI, and AD) in ^{18}F-AV-1451 binding values

	Onset age × Diagnosis	Onset age × MMSE
Global cortex	***0.011***	***0.001***
Prefrontal	0.230	***0.036***
Sensorimotor	0.061	***0.009***
Superior parietal	***0.001***	***< 0.001***
Inferior parietal	***0.001***	***< 0.001***
Precuneus	***0.016***	***0.003***
Occipital	***< 0.001***	***< 0.001***
Superior temporal	***0.010***	***0.004***
Middle temporal	0.065	***0.019***
Inferior temporal	***0.006***	***< 0.001***
Hippocampus	0.116	0.243
Entorhinal	0.103	0.073
Parahippocampal	***0.025***	***0.011***
Anterior cingulate	0.909	0.577
Posterior cingulate	0.079	***0.021***

Data are presented as *P*-values.

Abbreviations: AD = Alzheimer's disease; MCI = mild cognitive impairment, × = interaction between independent variables

3. Surface-based comparison of cortical ^{18}F-AV-1451 binding

Compared with YC, EOMCI patients showed mildly increased ^{18}F-AV-1451 binding in the bilateral medial temporal, left inferior parietal, left posterior cingulate and left precuneus cortices (uncorrected $P < 0.01$), but these regions did not survive multiple comparisons. Compared with OC, LOMCI patients showed mildly increased binding in the bilateral medial and lateral temporal, and right inferior parietal cortices (uncorrected $P < 0.01$), but only a small region in the left entorhinal cortex survived multiple comparisons. Compared with each control group, both EOAD and LOAD patients commonly showed increased binding in most of the cortical regions. In EOAD patients, increased binding was most prominent in the parieto-temporo-occipital cortices, while the left medial and inferior temporal cortices were most prominent in the LOAD patients (Fig. 1).

Compared with EOMCI, EOAD patients showed greater binding in most cortical regions with the greatest differences in the right parietal, precuneus, occipital, inferior temporal, and dorsolateral prefrontal cortices. The LOAD patients showed greater binding than LOMCI in the left lateral and medial temporal, precuneus, inferior parietal, and prefrontal cortex (Fig. 1).

Like VOI-based analysis, the EOMCI and LOMCI patients did not differ in terms of cortical ^{18}F-AV-1451 binding even with most liberal uncorrected $P < 0.05$. When compared to LOAD patients, the EOAD patients showed greater binding in the right inferior parietal, occipital, and inferior temporal cortices (Fig. 1).

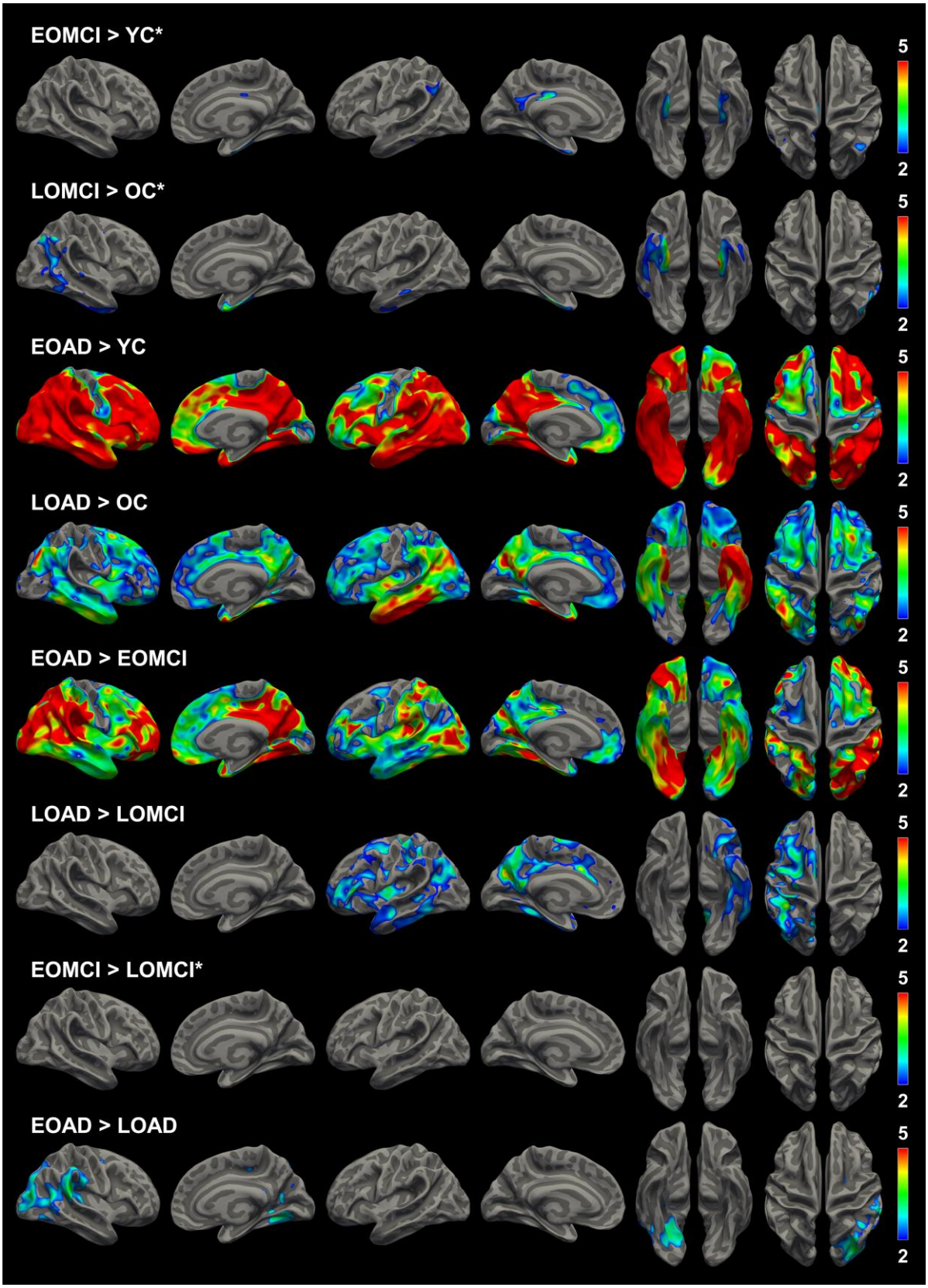

Fig. 1. Surface-based comparisons of ^{18}F-AV-1451 binding

EOMCI patients show mildly increased binding in the bilateral medial temporal, left inferior parietal, left posterior cingulate and left precuneus cortices with uncorrected $P < 0.01$, while increased binding in the left medial temporal cortex is prominent in LOMCI. Both EOAD and LOAD show prominently increased binding across the entire cerebral cortex, with EOAD showing a much greater difference compared to the controls. When compared to MCI, each AD group shows greater binding in the widespread cerebral cortex, and the difference is more prominent in the EOAD *vs.* EOMCI comparison. While no region exhibits a difference between EOMCI and LOMCI, EOAD shows greater binding than LOAD in the right parieto-occipital cortex.

Color bars represent $-\log_{10}$ *P*-value for group comparison.

Group comparison results uncorrected for multiple comparisons are marked with asterisks. In case of LOMCI vs. OC comparison, uncorrected result is displayed because very small region in the left entorhinal cortex survived multiple comparisons.

Abbreviations: EO = early-onset; LO = late-onset; AD = Alzheimer's disease; MCI = mild cognitive impairment; YC = young controls; OC = old controls

4. Association between cognitive function and cortical ^{18}F-AV-1451 binding

There were interactions for ^{18}F-AV-1451 binding between the onset age and MMSE scores in most of the regions except for the hippocampus, entorhinal, and anterior cingulate cortices (Table 3), and levels of cortical ^{18}F-AV-1451 binding increased as cognitive dysfunction worsened (Table 4, Fig. 2 and 3).

Data for EOAD/MCI and LOAD/MCI patients showed significant negative correlation between ^{18}F-AV-1451 binding in the global cerebral cortex and global cognitive assessments such as MMSE score (Table 4, Fig. 3A and 3D). The EOAD/MCI patients showed correlation in much wider parieto-temporo-occipital cortices than the LOAD/MCI patients (Table 4, Fig. 2).

We investigated the particular regions with increasing tau accumulation that were associated with worsening of a specific cognitive domain. In the EOAD/MCI patients, the worsening of visuospatial function measured by RCFT was associated with an increase in ^{18}F-AV-1451 binding in the superior and inferior parietal, precuneus, and occipital cortices ($P < 0.005$), which survived region-wise multiple comparisons (Table 4, Fig. 3B and 3E), and the correlation was more prominent in the parieto-occipital cortex of the right hemisphere (Fig. 2). In contrast, in the LOAD/MCI patients, the worsening of verbal memory function measured by SVLT-DR was associated with an increase in binding in the middle and inferior temporal, entorhinal, and parahippocampal cortices ($P < 0.01$), which survived multiple comparisons (Table 4, Fig. 3C and 3F). However, those regions did not survive multiple comparisons in surface-based analysis (Fig. 2).

Table 4. Correlation between the ^{18}F-AV-1451 binding values and cognition in early- and late-onset patients with Alzheimer's disease spectrum

	EOAD/MCI						
	MMSE	**DS-BW**	**BNT**	**RCFT**	**SVLT-DR**	**RCFT-DR**	**COWAT**
Prefrontal	***-0.667[b]***	-0.357	0.046	-0.300	-0.338	-0.282	0.130
Superior parietal	***-0.742[b]***	-0.514[a*]	-0.128	***-0.630[b]***	-0.242	-0.219	-0.005
Inferior parietal	***-0.717[b]***	-0.438[a*]	-0.020	***-0.589[b]***	-0.238	-0.205	0.103
Precuneus	***-0.652[b]***	-0.480[a*]	0.041	***-0.606[b]***	-0.266	-0.272	-0.010
Occipital	***-0.778[b]***	-0.166	-0.197	***-0.583[b]***	-0.260	-0.220	-0.124
Superior temporal	***-0.709[b]***	-0.114	-0.029	-0.391	-0.203	-0.201	0.119
Middle temporal	***-0.711[b]***	-0.260	0.010	-0.349	-0.296	-0.223	0.083
Inferior temporal	***-0.834[b]***	-0.368	-0.118	-0.444[a*]	-0.253	-0.175	0.101
Hippocampus	-0.401	-0.087	0.475[a*]	0.219	-0.430	-0.524[a*]	0.165
Entorhinal	***-0.674[b]***	-0.058	0.138	0.084	-0.557[b*]	-0.492[a*]	0.323
Parahippocampal	***-0.800[b]***	-0.211	0.168	-0.180	-0.495[a*]	-0.491[a*]	0.245
Anterior cingulate	***-0.599[b]***	-0.121	0.114	-0.066	-0.297	-0.229	0.052
Posterior cingulate	***-0.664[b]***	-0.388	0.123	-0.493[a*]	-0.285	-0.310	0.062
	LOAD/MCI						
	MMSE	**DS-BW**	**BNT**	**RCFT**	**SVLT-DR**	**RCFT-DR**	**COWAT**
Prefrontal	***-0.382[a]***	0.279	-0.043	0.281	-0.162	-0.005	-0.238
Superior parietal	***-0.585[b]***	0.063	-0.160	0.015	0.147	-0.070	-0.204
Inferior parietal	***-0.539[b]***	0.374[a*]	-0.154	0.182	-0.151	-0.091	-0.246
Precuneus	***-0.507[b]***	0.271	0.001	0.263	-0.161	-0.085	-0.352[a*]
Occipital	***-0.398[a]***	0.276	-0.221	0.396[a*]	-0.077	-0.192	-0.186
Superior temporal	-0.346[a*]	0.427[b*]	-0.256	0.291	-0.370[a*]	-0.142	-0.218
Middle temporal	-0.337[a*]	0.386[a*]	-0.215	0.341[a*]	***-0.439[b]***	-0.175	-0.290
Inferior temporal	-0.343[a*]	0.396[a*]	-0.377[a*]	0.262	***-0.424[b]***	-0.214	-0.240
Hippocampus	-0.119	0.324[a*]	-0.174	0.073	-0.296	-0.316	-0.227
Entorhinal	-0.189	0.130	-0.247	0.196	***-0.428[b]***	-0.427[b*]	-0.336[a*]
Parahippocampal	-0.249	0.342[a*]	-0.332[a*]	0.204	***-0.442[b]***	-0.410[a*]	-0.322[a*]
Anterior cingulate	***-0.368[a]***	0.299	0.014	0.329[a*]	-0.195	-0.068	-0.319
Posterior cingulate	***-0.403[a]***	0.283	0.021	0.280	-0.294	-0.189	-0.392[a*]

[a]$P < 0.05$, [b]$P < 0.01$; [*]Region did not survive region-wise correction for multiple comparisons.

Correlation analyses between the binding values and the global cognitive scales (CDR-SB and MMSE scores) were performed after controlling for age and education in early and late onset patients with Alzheimer's disease spectrum, respectively. The correlation analyses of the tests for each cognitive domain were performed after controlling for age and years of education and global cognitive scale (MMSE score) as well. Data are presented with correlation coefficients.

Abbreviations: EO = early-onset; LO = late-onset; AD = Alzheimer's disease; MCI = mild cognitive impairment;; MMSE = Mini-Mental State Examination; DS-BW = Digit Span Backward; BNT = Boston Naming Test; RCFT = Rey-Osterrieth Complex Figure Test; SVLT-DR = Seoul Verbal Learning Test-Delayed Recall; RCFT-DR = Rey-Osterrieth Complex Figure Test-Delayed Recall; COWAT = Controlled Oral Word Association Test-Semantics

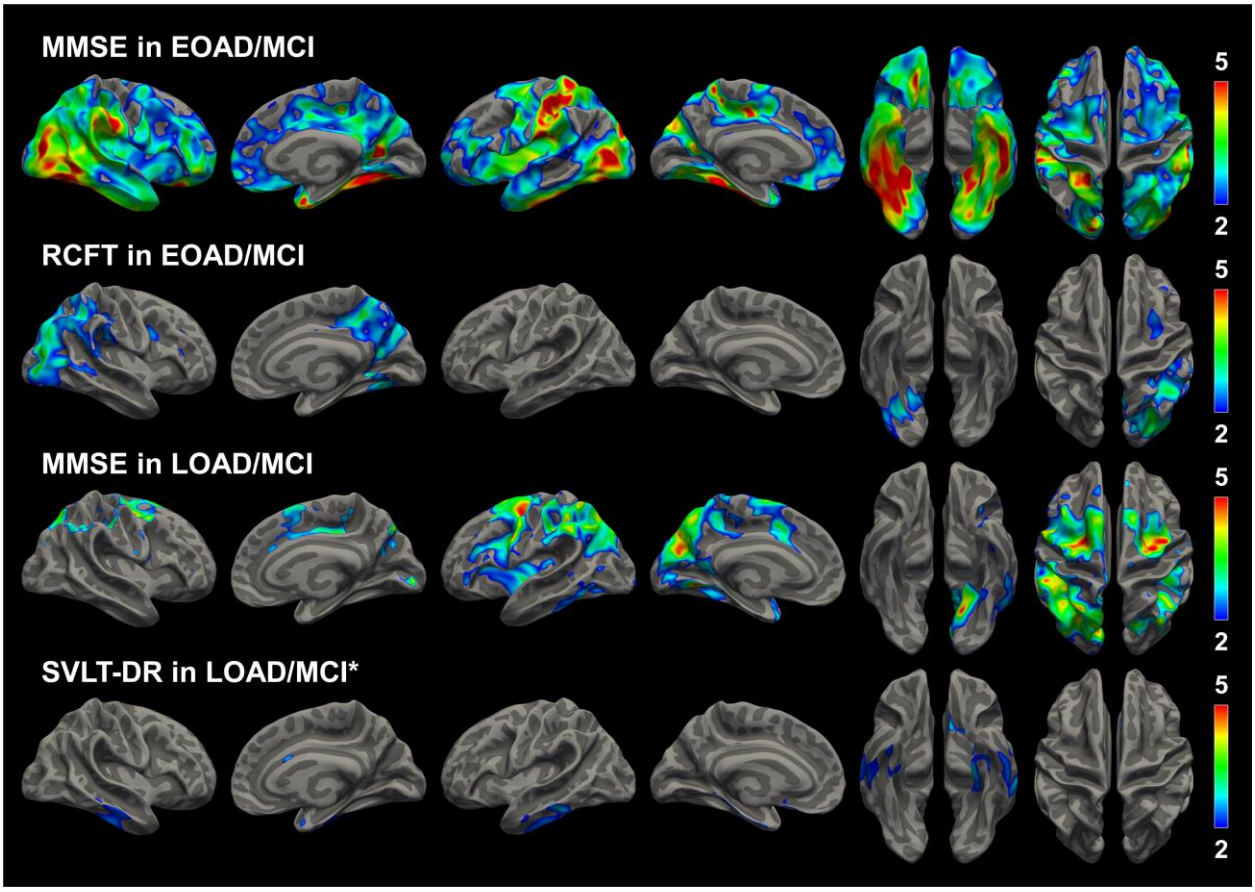

Fig. 2. Surface-based correlation analysis between ^{18}F-AV-1451 binding and cognition in early- and late-onset patients with Alzheimer's disease spectrum

Both EOAD/MCI and LOAD/MCI groups show a negative correlation between the MMSE scores and ^{18}F-AV-1451 binding in the widespread cerebral cortex. EOAD/MCI patients showed correlation in much wider parieto-temporo-occipital cortices than the LOAD/MCI patients. The visuospatial dysfunction is related to the ^{18}F-AV-1451 binding in the right parieto-occipital cortex of EOAD/MCI. Verbal memory dysfunction is related to binding in the medial and inferior temporal cortices of LOAD/MCI, but this correlation did not survive multiple comparisons.

Color bars represent -$\log_{10}$ *P*-value.

Result uncorrected for multiple comparisons is marked with asterisk.

Abbreviations: EO = early-onset; LO = late-onset; AD/MCI = Alzheimer's disease spectrum; MMSE = Mini-Mental State Examination; RCFT = Rey-Osterrieth Complex Figure Test; SVLT-DR = Seoul Verbal Learning Test-Delayed Recall

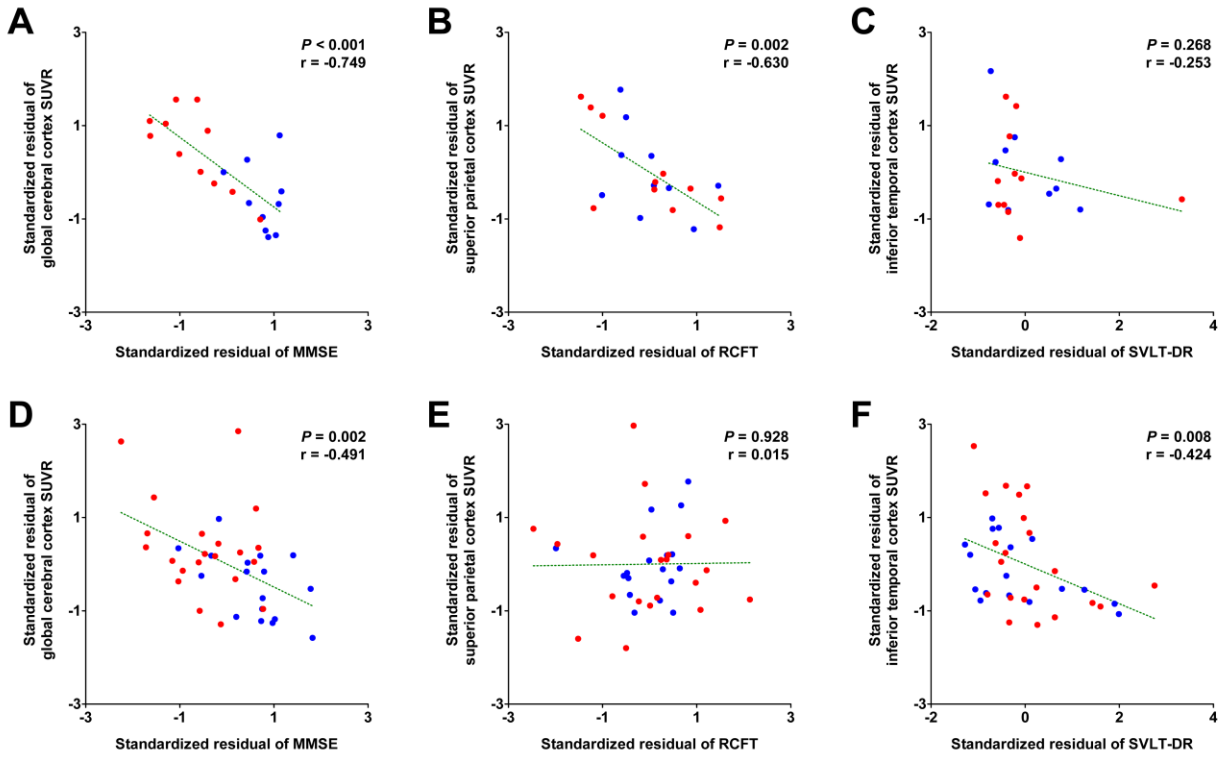

Fig. 3. Correlation between ^{18}F-AV-1451 binding values and cognition in early- and late-onset patients with Alzheimer's disease spectrum

Correlation analysis was performed in EOAD/MCI (A, B, and C) and LOAD/MCI (D, E, and F) groups separately. For global cognition (MMSE; A and D), the values were adjusted for age and years of education. For the visuospatial (RCFT; B and E) and verbal memory functions (SVLT-DR; C and F), the values were adjusted for age, years of education and global cognition. Blue dots represent MCI patients and red dots represent AD patients.

Abbreviations: AD = Alzheimer's disease; MCI = mild cognitive impairment; CDR-SB = Clinical Dementia Rating sum-of-boxes; r = correlation coefficient; SUVR = standardized uptake value ratio

5. Comparison of cortical ^{18}F-florbetaben binding and correlation with cognitive function

Regional SUVR values for ^{18}F-florbetaben PET and the statistical results are summarized in Table 5. There were no differences in ^{18}F-florbetaben binding between EOMCI and LOMCI or between the EOAD and LOAD patients. Even after lowering the cut-off onset age to 62 years, also there was no difference in binding between the EOMCI and LOMCI patients and between the EOAD and LOAD patients as well.

Unlike the close relationship between the severity of global cognitive dysfunction and cortical ^{18}F-AV-1451 binding, ^{18}F-florbetaben binding did not correlate with MMSE scores in either EOAD/MCI or LOAD/MCI patients. Moreover, regional ^{18}F-florbetaben binding did not correlate with any cognitive domains tested in either of the AD/MCI groups.

Table 5. Comparison of ^{18}F-florbetaben binding values between the diagnostic groups

	SUVR			*P*-value			
	EOAD	**EOMCI**	**YC**	**EOAD > YC**	**EOMCI > YC**	**EOAD > EOMCI**	**EOMCI > LOMCI**
Global cortex	1.89±0.19	1.65±0.21	1.23±0.06	***< 0.001***	***< 0.001***	***0.009***	0.998
Prefrontal	2.07±0.22	1.76±0.26	1.28±0.08	***< 0.001***	***< 0.001***	***0.003***	0.590
Sensorimotor	1.74±0.20	1.59±0.16	1.28±0.07	***< 0.001***	***< 0.001***	0.118	0.785
Superior parietal	1.83±0.25	1.62±0.23	1.22±0.08	***< 0.001***	***< 0.001***	0.082	0.925
Inferior parietal	1.93±0.24	1.69±0.24	1.21±0.09	***< 0.001***	***< 0.001***	0.038*	0.872
Precuneus	2.16±0.31	1.86±0.32	1.26±0.10	***< 0.001***	***< 0.001***	0.057	0.895
Occipital	1.69±0.23	1.50±0.16	1.21±0.06	***< 0.001***	***< 0.001***	0.046*	0.815
Superior temporal	1.79±0.21	1.59±0.27	1.14±0.06	***< 0.001***	***< 0.001***	0.141	0.387
Middle temporal	1.74±0.16	1.56±0.24	1.12±0.07	***< 0.001***	***< 0.001***	0.069	0.617
Inferior temporal	1.79±0.18	1.55±0.22	1.13±0.05	***< 0.001***	***< 0.001***	***0.007***	0.732
Hippocampus	1.34±0.13	1.33±0.13	1.29±0.05	0.993	> 0.999	> 0.999	0.314
Entorhinal	1.27±0.14	1.22±0.14	1.09±0.05	***0.001***	***0.026***	0.899	0.972
Parahippocampal	1.58±0.17	1.42±0.16	1.14±0.05	***< 0.001***	***< 0.001***	0.055	0.578
Anterior cingulate	2.27±0.24	1.87±0.28	1.38±0.12	***< 0.001***	***< 0.001***	***0.001***	0.643
Posterior cingulate	2.13±0.24	1.85±0.27	1.35±0.10	***< 0.001***	***< 0.001***	0.021*	0.633
	SUVR			***P*-value**			
	LOAD	**LOMCI**	**OC**	**LOAD > OC**	**LOMCI > OC**	**LOAD > LOMCI**	**EOAD > LOAD**
Global cortex	1.87±0.31	1.62±0.28	1.20±0.05	***< 0.001***	***< 0.001***	***0.004***	0.304
Prefrontal	2.08±0.37	1.79±0.37	1.24±0.04	***< 0.001***	***< 0.001***	***0.009***	0.205
Sensorimotor	1.80±0.35	1.54±0.28	1.24±0.05	***< 0.001***	***0.009***	***0.010***	0.107
Superior parietal	1.88±0.39	1.60±0.29	1.14±0.05	***< 0.001***	***< 0.001***	***0.010***	0.208
Inferior parietal	1.91±0.33	1.64±0.31	1.17±0.08	***< 0.001***	***< 0.001***	***0.005***	0.341
Precuneus	2.24±0.45	1.85±0.38	1.22±0.05	***< 0.001***	***< 0.001***	***0.002***	0.131
Occipital	1.66±0.28	1.47±0.20	1.19±0.06	***< 0.001***	***0.002***	***0.023***	0.751
Superior temporal	1.72±0.27	1.48±0.28	1.13±0.07	***< 0.001***	***< 0.001***	***0.003***	0.808
Middle temporal	1.70±0.27	1.49±0.25	1.12±0.05	***< 0.001***	***< 0.001***	***0.006***	0.614
Inferior temporal	1.70±0.27	1.50±0.24	1.15±0.05	***< 0.001***	***< 0.001***	***0.011***	0.913
Hippocampus	1.24±0.15	1.25±0.17	1.23±0.11	> 0.999	> 0.999	> 0.999	0.114
Entorhinal	1.26±0.19	1.20±0.17	1.08±0.07	***0.002***	0.134	0.318	0.580
Parahippocampal	1.53±0.22	1.37±0.18	1.13±0.05	***< 0.001***	***0.001***	***0.010***	0.951
Anterior cingulate	2.22±0.39	1.89±0.42	1.34±0.08	***< 0.001***	***< 0.001***	***0.006***	0.542
Posterior cingulate	2.20±0.38	1.88±0.38	1.30±0.06	***< 0.001***	***< 0.001***	***0.006***	0.123

*Regions did not survive region-wise correction for multiple comparisons.

Data are presented as mean ± SD.

Abbreviations: SUVR = standardized uptake value ratio; EO = early-onset; LO = late-onset; AD = Alzheimer's disease; MCI = mild cognitive impairment; YC = young controls; OC = old controls

Ⅳ. DISCUSSION

In this study, we found that EOAD patients showed greater tau binding most prominently in the superior and inferior parietal, and occipital cortices than LOAD patients. Tau accumulation in the right parieto-occipital cortex of EOAD/MCI patients was closely associated with visuospatial dysfunction, and that in the basal, lateral and medial temporal cortices of LOAD/MCI was associated with verbal memory dysfunction. To our knowledge, this represents the first in vivo evidence that EOAD is associated with greater tau accumulation in regions topographically distinct from LOAD.

In contrast to this clear difference in cortical tau accumulation, we could not find any difference in cortical ^{18}F-florbetaben binding between the EOAD and LOAD patients. This result is in agreement with the previous report showing no difference in ^{11}C-PIB binding between two groups separated by an age cut-off of 65 years at onset [7,13]. Unlike these in vivo PET studies, postmortem studies have consistently reported greater amyloid plaque load in the neocortex of EOAD patients [10,11,30,31]. Rabinovici et al. explained this discrepancy as being due to the limitations of such postmortem studies (e.g. an inability to match dementia severity, the tendency to include patients at advanced stages, and a lack of consideration for comorbid pathology and plaque morphology) [7]. In addition, because we selectively included only the amyloid-positive MCI and AD patients, amyloid load might have been biased. Although one study categorizing AD patients into younger and older groups with an age cut-off of 62 years at diagnosis showed greater ^{11}C-PIB binding in the parietal cortex of the younger AD patients and correlation between the parietal amyloid-β load and visuospatial dysfunction [12], amyloid-β pathology might have much lower impact on the distinct clinical characteristics of EOAD patients than tau pathology.

In AD, tau accumulation first appears in the transentorhinal region, and spreads first to the neighboring limbic and basal temporal regions [32]. Subsequently, the posterior cingulate, precuneus and the inferior parietal cortices distant from the medial temporal cortex are likely to be affected by tau accumulation [15-17,32]. These regions form a posterior default mode network (DMN) shown in resting state functional MR imaging studies [33]. The anterior DMN increases with aging in healthy controls, while the posterior DMN decreases. Interestingly, AD patients showed greater age-related change in DMN [34]. Relatively preserved functional network of posterior DMN in younger individuals compared to the elderly might serve as a faster route for the propagation of tau pathology. This may partly explain the greater tau burden in EOAD patients, particularly in the parieto-occipital cortices.

Another hypothesis that may explain the greater tau burden in EOAD patients is neuroinflammation. In a postmortem study of AD, microgliosis correlated with NFT pathology and steadily increased, even after the plateauing of amyloid plaque load [35]. Recent animal model studies have shown that microglia drive the production and propagation of pathological tau protein and these responses

can be blocked by immunosuppressants or deletion of microglia [36-38]. These findings suggest that neuroinflammation may play an important role in the initiation of tau pathology and disease progression in AD. A PET study of neuroinflammation using ^{11}C-PBR28 showed increased neuroinflammation in the prefrontal, inferior and superior parietal, precuneus, posterior cingulate, occipital, and lateral and medial temporal cortices in AD patients, but not in MCI patients. Interestingly, EOAD patients showed greater neuroinflammation in the prefrontal, inferior parietal, precuneus, and occipital cortices when compared to LOAD patients [39]. These regions closely resemble the cortical regions with a prominent accumulation of tau in our EOAD patients. Greater tau burden in EOAD patients may therefore be partly explained by increased neuroinflammation.

In this study, we found that the tau accumulation in different regions was associated with specific cognitive dysfunction in EOAD/MCI and LOAD/MCI patients. Those regions correspond to the regions responsible for each cognitive function affected [12], and specific cognitive dysfunction may be predicted by topographic distribution of tau as shown in a ^{18}F-AV-1451 PET study in patients with focal variants of Alzheimer's disease, such as posterior cortical atrophy or logopenic aphasia [40].

It is notable that the EOAD patients showed greatly increased ^{18}F-AV-1451 binding than the LOAD patients, despite there being no difference between the EOMCI and LOMCI patients. We cautiously suspect that the accumulation of tau could be accelerated from the period of clinical conversion to dementia in EOAD patients. An ^{18}F-fluorodeoxyglucose PET study showed that the hypometabolic regions prominently increased at an early stage in EOAD patients compared to LOAD patients [8], and the EOAD patients showed more rapid progression of cognitive dysfunctions and greater cortical thinning in the widespread association cortices than the LOAD patients in a 3-years longitudinal study [9]. These results may support the hypothesis of accelerated tau accumulation in EOAD.

Ⅴ. CONCLUSION

The EOAD patients had greater tau accumulation with different topography compared to the LOAD patients. Excessive tau accumulation in the parieto-occipital cortex of EOAD patients may explain clinical characteristics that are distinct from LOAD patients. A longitudinal study with more number of EOAD patients will be required to determine whether the rate of tau accumulation is accelerated in EOAD patients.

REFERENCES

1. Werner P, Stein-Shvachman I, Korczyn AD. Early onset dementia: clinical and social aspects. *Int Psychogeriatr* 2009; 21(4): 631-6.

2. Heyman A, Wilkinson WE, Hurwitz BJ, et al. Early-onset Alzheimer's disease: clinical predictors of institutionalization and death. *Neurology* 1987; 37(6): 980-4.

3. Koss E, Edland S, Fillenbaum G, et al. Clinical and neuropsychological differences between patients with earlier and later onset of Alzheimer's disease: A CERAD analysis, Part XII. *Neurology* 1996; 46(1): 136-41.

4. Jacobs D, Sano M, Marder K, et al. Age at onset of Alzheimer's disease: relation to pattern of cognitive dysfunction and rate of decline. *Neurology* 1994; 44(7): 1215-20.

5. Frisoni GB, Pievani M, Testa C, et al. The topography of grey matter involvement in early and late onset Alzheimer's disease. *Brain : a journal of neurology* 2007; 130(Pt 3): 720-30.

6. Smits LL, Pijnenburg YA, Koedam EL, et al. Early onset Alzheimer's disease is associated with a distinct neuropsychological profile. *J Alzheimers Dis* 2012; 30(1): 101-8.

7. Rabinovici GD, Furst AJ, Alkalay A, et al. Increased metabolic vulnerability in early-onset Alzheimer's disease is not related to amyloid burden. *Brain : a journal of neurology* 2010; 133(Pt 2): 512-28.

8. Kim EJ, Cho SS, Jeong Y, et al. Glucose metabolism in early onset versus late onset Alzheimer's disease: an SPM analysis of 120 patients. *Brain : a journal of neurology* 2005; 128(Pt 8): 1790-801.

9. Cho H, Jeon S, Kang SJ, et al. Longitudinal changes of cortical thickness in early- versus late-onset Alzheimer's disease. *Neurobiology of aging* 2013; 34(7): 1921 e9- e15.

10. Hansen LA, DeTeresa R, Davies P, Terry RD. Neocortical morphometry, lesion counts, and choline acetyltransferase levels in the age spectrum of Alzheimer's disease. *Neurology* 1988; 38(1): 48-54.

11. Ho GJ, Hansen LA, Alford MF, et al. Age at onset is associated with disease severity in Lewy body variant and Alzheimer's disease. *Neuroreport* 2002; 13(14): 1825-8.

12. Ossenkoppele R, Zwan MD, Tolboom N, et al. Amyloid burden and metabolic function in early-onset Alzheimer's disease: parietal lobe involvement. *Brain : a journal of neurology* 2012; 135(Pt 7): 2115-25.

13. Cho H, Seo SW, Kim JH, et al. Amyloid deposition in early onset versus late onset Alzheimer's disease. *J Alzheimers Dis* 2013; 35(4): 813-21.

14. Marquie M, Normandin MD, Vanderburg CR, et al. Validating novel tau positron emission tomography tracer [F-18]-AV-1451 (T807) on postmortem brain tissue. *Ann Neurol* 2015; 78(5): 787-800.

15. Johnson KA, Schultz A, Betensky RA, et al. Tau positron emission tomographic imaging in aging and early Alzheimer disease. *Ann Neurol* 2016; 79(1): 110-9.

16. Schwarz AJ, Yu P, Miller BB, et al. Regional profiles of the candidate tau PET ligand 18F-AV-1451 recapitulate key features of Braak histopathological stages. *Brain : a journal of neurology* 2016; 139(Pt 5): 1539-50.

17. Cho H, Choi JY, Hwang MS, et al. In vivo cortical spreading pattern of tau and amyloid in the Alzheimer disease spectrum. *Ann Neurol* 2016; 80(2): 247-58.

18. McKhann G, Drachman D, Folstein M, Katzman R, Price D, Stadlan EM. Clinical diagnosis of Alzheimer's disease: report of the NINCDS-ADRDA Work Group under the auspices of Department of Health and Human Services Task Force on Alzheimer's Disease. *Neurology* 1984; 34(7): 939-44.

19. Petersen RC, Smith GE, Waring SC, Ivnik RJ, Tangalos EG, Kokmen E. Mild cognitive impairment: clinical characterization and outcome. *Arch Neurol* 1999; 56(3): 303-8.

20. Fazekas F, Chawluk JB, Alavi A, Hurtig HI, Zimmerman RA. MR signal abnormalities at 1.5 T in Alzheimer's dementia and normal aging. *AJR Am J Roentgenol* 1987; 149(2): 351-6.

21. Sabri O, Sabbagh MN, Seibyl J, et al. Florbetaben PET imaging to detect amyloid beta plaques in Alzheimer's disease: phase 3 study. *Alzheimers Dement* 2015; 11(8): 964-74.

22. Villemagne VL, Ong K, Mulligan RS, et al. Amyloid imaging with (18)F-florbetaben in Alzheimer disease and other dementias. *J Nucl Med* 2011; 52(8): 1210-7.

23. Ahn HJ, Chin J, Park A, et al. Seoul Neuropsychological Screening Battery-dementia version (SNSB-D): a useful tool for assessing and monitoring cognitive impairments in dementia patients. *Journal of Korean medical science* 2010; 25(7): 1071-6.

24. Kang Y, Na DL. Seoul Neuropsychological Screening Battery (SNSB). Incheon, South Korea: Human Brain Research & Consulting Co.; 2003.

25. Fischl B, Salat DH, Busa E, et al. Whole brain segmentation: automated labeling of neuroanatomical structures in the human brain. *Neuron* 2002; 33(3): 341-55.

26. Desikan RS, Segonne F, Fischl B, et al. An automated labeling system for subdividing the human cerebral cortex on MRI scans into gyral based regions of interest. *NeuroImage* 2006; 31(3): 968-80.

27. Fischl B, van der Kouwe A, Destrieux C, et al. Automatically parcellating the human cerebral cortex. *Cerebral cortex* 2004; 14(1): 11-22.

28. Thomas BA, Erlandsson K, Modat M, et al. The importance of appropriate partial volume correction for PET quantification in Alzheimer's disease. *European journal of nuclear medicine and molecular imaging* 2011; 38(6): 1104-19.

29. Benjamini Y, Hochberg Y. Controlling the false discovery rate: a practical and powerful approach to multiple testing. *Journal of the Royal Statistical Society B* 1995; 57(1): 289-300.

30. Bigio EH, Hynan LS, Sontag E, Satumtira S, White CL. Synapse loss is greater in presenile than senile onset Alzheimer disease: implications for the cognitive reserve hypothesis. *Neuropathol Appl Neurobiol* 2002; 28(3): 218-27.

31. Marshall GA, Fairbanks LA, Tekin S, Vinters HV, Cummings JL. Early-onset Alzheimer's disease is associated with greater pathologic burden. *J Geriatr Psychiatry Neurol* 2007; 20(1): 29-33.

32. Braak H, Braak E. Neuropathological stageing of Alzheimer-related changes. *Acta Neuropathol* 1991; 82(4): 239-59.

33. Buckner RL, Andrews-Hanna JR, Schacter DL. The brain's default network: anatomy, function, and relevance to disease. *Ann N Y Acad Sci* 2008; 1124: 1-38.

34. Jones DT, Machulda MM, Vemuri P, et al. Age-related changes in the default mode network are more advanced in Alzheimer disease. *Neurology* 2011; 77(16): 1524-31.

35. Serrano-Pozo A, Mielke ML, Gomez-Isla T, et al. Reactive glia not only associates with plaques but also parallels tangles in Alzheimer's disease. *Am J Pathol* 2011; 179(3): 1373-84.

36. Asai H, Ikezu S, Tsunoda S, et al. Depletion of microglia and inhibition of exosome synthesis halt tau propagation. *Nat Neurosci* 2015; 18(11): 1584-93.

37. Maphis N, Xu G, Kokiko-Cochran ON, et al. Reactive microglia drive tau pathology and contribute to the spreading of pathological tau in the brain. *Brain : a journal of neurology* 2015; 138(Pt 6): 1738-55.

38. Yoshiyama Y, Higuchi M, Zhang B, et al. Synapse loss and microglial activation precede tangles in a P301S tauopathy mouse model. *Neuron* 2007; 53(3): 337-51.

39. Kreisl WC, Lyoo CH, McGwier M, et al. In vivo radioligand binding to translocator protein correlates with severity of Alzheimer's disease. *Brain : a journal of neurology* 2013; 136(Pt 7): 2228-38.

40. Ossenkoppele R, Schonhaut DR, Scholl M, et al. Tau PET patterns mirror clinical and neuroanatomical variability in Alzheimer's disease. *Brain : a journal of neurology* 2016; 139(Pt 5): 1551-67.

ABSTRACT (IN KOREAN)

조기발현형 알츠하이머 병에서 나타나는 특징적인 두정-후두엽 피질의 과도한 타우 축적 양상

<지도교수 최 영 철>

연세대학교 대학원 의학과

조 한 나

서론: 조기발현형 알츠하이머병은 만기발현형 알츠하이머병에 비해 기억력을 제외한 다양한 인지기능의 장애, 급격한 진행 경과, 더 심각한 뇌피질의 대사량 저하 및 위축을 특징을 보이나, 이전의 아밀로이드 페트 검사에서는 두 군간의 비교적 비슷한 아밀로이드의 축적양상을 보였다. 본 연구에서는 조기발현형과 만기발현형 알츠하이머 치매와 경도인지장애 환자군을 통해 타우 단백의 축적 정도를 비교하고 질병 발생 시점에 따라 타우 축적 패턴이 다른지 확인하고자 하였다.

방법: 총 90 명의 경도 및 중증도 단계의 알츠하이머 치매와 경도인지장애 환자를 등록하였으며 모든 환자들은 타우 페트와 아밀로이드 페트 뇌영상 검사를 시행하였다. 이 중에서 아밀로이드 페트 검사상 양성인 총 59 명의 환자들을 대상으로 증상 발생나이 65 세를 기준으로 조기발현형과 만기발현형을 분류하였다 (11 명의 조기발현형-알츠하이머병, 10 명의 조기발현형-경도인지장애, 21 명의 만기발현형-알츠하이머병, 17 명의 만기발현형-경도인지장애). 그리고 대조군으로 각각 환자군의 나이에 맞는 아밀로이드 음성 정상인 군을 각각 15 명씩 등록하였다.

결과: 정상대조군에 비해 조기발현형과 만기발현형 알츠하이머 치매군은 뚜렷하게 증가된 타우축적을 광범위한 뇌피질영역에서 관찰할 수 있었다. 조기발현형과 만기발현형 경도인지장애군 사이의 맞비교 분석에서는 유의한 타우 축적의 차이는 관찰되지 않았으나, 조기발현형과 만기발현형 알츠하이머 치매군간의 맞비교 분석에서는 조기발현형 알츠하이머 치매군이 만기발현형 알츠하이머 치매군보다 두정-후두엽 지역의 타우 축적이 더 뚜렷하게 관찰되었다. 특히 두정-후두엽의 타우축적 정도와 시공간능력이 조기발현형 알츠하이머치매

및 경도인지장애 환자군 안에서 유의한 상관관계를 나타냈으며, 만기발현형 알츠하이머치매 및 경도인지장애 환자군 안에서는 측두엽의 타우 축적 정도와 언어적 기억력이 유의한 상관관계를 보였다.

결론: 조기발현형 알츠하이머 치매환자군은 만기발현형 알츠하이머 치매환자군에 비해 더 심각한 타우 축적이 관찰되었으며, 특히 두정-후두엽 지역의 타우 축적이 뚜렷이 관찰되었다. 이 결과를 비추어 볼 때 명확히 다른 타우축적 양상의 차이가 증상 발생 시점에 따른 인지기능 및 진행경과의 차이를 반영하는 중요한 인자가 됨을 알 수 있었다.

핵심되는 말: 알츠하이머병, 경도인지장애, 조기발현형, 타우, 양전자방출 단층촬영

PUBLICATION LIST

1. Cho H, Choi JY, Lee SH, et al. Excessive tau accumulation in the parieto-occipital cortex characterizes early-onset Alzheimer's disease. Neurobiol Aging 2017; 53:103-111.